Mass Diffusion and Thermal Diffusivity of the Decane-pentane Mixture Under High Pressure as a Ground-based Study for SCCO Project

I. Lizarraga, C. Giraudet, Fabrizio Croccolo, M.M. Bou-Ali, Henri Bataller

▶ **To cite this version:**

I. Lizarraga, C. Giraudet, Fabrizio Croccolo, M.M. Bou-Ali, Henri Bataller. Mass Diffusion and Thermal Diffusivity of the Decane-pentane Mixture Under High Pressure as a Ground-based Study for SCCO Project. Microgravity Science and Technology, Springer, 2016, 28 (5), pp.545-552. 10.1007/s12217-016-9506-9 . hal-01815883

HAL Id: hal-01815883

https://hal.archives-ouvertes.fr/hal-01815883

Submitted on 6 Feb 2020

HAL is a multi-disciplinary open access archive for the deposit and dissemination of scientific research documents, whether they are published or not. The documents may come from teaching and research institutions in France or abroad, or from public or private research centers.

L'archive ouverte pluridisciplinaire **HAL**, est destinée au dépôt et à la diffusion de documents scientifiques de niveau recherche, publiés ou non, émanant des établissements d'enseignement et de recherche français ou étrangers, des laboratoires publics ou privés.

Manuscript Click here to download Manuscript ELGRA_scco_re_rev.docx

Mass diffusion and thermal diffusivity of the decane-pentane mixture under high pressure as a ground-based study for SCCO project

Ion Lizarraga[1], Cédric Giraudet[2], Fabrizio Croccolo[2], M. Mounir Bou-Ali[1], and Henri Bataller[2]

[1] *MGEP Mondragon Goi Eskola Politeknikoa, Mechanical and Industrial Manufacturing Department, Loramendi 4 Apdo. 23, 20500 Mondragon, Spain*

[2] *Laboratoire des Fluides Complexes et leurs Réservoirs, UMR-5150, Université de Pau et des Pays de l'Adour, 1 Allée du Parc Montaury, Anglet, FR.*

Abstract

Thermodiffusion experiments on iso-massic binary mixture of decane and pentane in the liquid phase have been performed between 25°C and 50°C and for pressures from 1MPa until 20MPa. By dynamic analysis of the light scattered by concentration non-equilibrium fluctuations in the binary mixture we obtained the mass diffusion coefficients of the mixture at each temperature and pressure. For the first time we were able to apply similar analysis to thermal fluctuations thus getting a simultaneous measurement of the thermal diffusivity coefficient. While mass diffusion coefficients decrease linearly with the pressure, thermal diffusivity coefficients increase linearly. In principle the proposed method can be used also for measuring the Soret coefficients at the same time. However, for the present mixture the intensity of the optical signal is limited by the optical contrast factor. This affects our capability of providing a reliable estimate of the Soret coefficient by means of dynamic Shadowgraph. Therefore the mass diffusion coefficients measurements would need to be combined with independent measurements of the thermodiffusion coefficients, e.g. thermogravitational column, to provide Soret coefficients. The obtained values constitute the

on-ground reference measurements for one of the mixture studied in the frame of the project SCCO-SJ10, which aims to measure the Soret coefficients of multicomponents mixtures under reservoir conditions. Microgravity experiments will be performed on the Chinese satellite SJ10 launched in April 2016.

Keywords: mass diffusion, thermal diffusivity, decane-pentane mixture, non-equilibrium fluctuations, high pressure, SCCO, SJ10

1. Introduction

The precise modelling of the distribution of chemical species in oil and gas reservoirs remains a topical issue for the oil industry, especially now that the reserves of fossil fuels are getting more difficult to extract. It is known that not only gravitational segregation, but also thermodiffusion due to geothermal gradients, are two physical phenomena determining the vertical distribution of species in hydrocarbon reservoirs on Earth (Lira-Galeana et al. 1994, Høier et al. 2001, Ghorayeb et al. 2003, Montel et al. 2007). Thermodiffusion, or Soret effect, is a phenomenon that couples heat and mass fluxes (de Groot and Mazur 1984) and can also lead to convective unstable conditions in particular cases (Galliero et al. 2009). The contribution of thermodiffusion is difficult to quantify, mainly due to a lack of experimental data as well as accurate modeling for multicomponent mixtures. Although noticeable progresses have been made during the last twenty years, (Assael et al., 2014 and references therein) especially on ternary mixtures both theoretically (Firoozabadi et al., 2000; Kempers, 2001; Galliero et al., 2003) and experimentally (Leahy-Dios et al., 2005; Larrañaga et al., 2015; Gebhardt et al., 2015), more work is necessary. Micro-gravity experiments, to avoid gravity-induced convection, are one possible way to provide further data on thermodiffusion in multicomponent mixtures (Georis et al., 1998; Van Vaerenbergh et al., 2009; Touzet et al., 2011; Bou-Ali et al., 2015). The Soret Coefficients in Crude Oil (SCCO) project aims at producing values of Soret coefficients of mixture of petroleum interest and in reservoirs conditions. In a first phase carried out in 2007 microgravity experiments were performed on board the Russian satellite FOTON-M3. One binary, two ternaries and one quaternary mixtures were studied (Van Vaerenbergh et al., 2009; Srinivasan et al., 2009; Touzet et al., 2011). The measurements were compared with molecular dynamics simulations and with theoretical calculations based on the Thermodynamics of Irreversible Processes. However, the conclusions were incomplete because of difficulties encountered during post flight analysis at

58 the laboratories (Touzet et al., 2011). Now, on the occasion of the China Sea well
59 explorations, a second phase of the SCCO space experiment has been scheduled. The
60 thermodiffusion behaviour of the binary mixture decane-pentane, the ternary mixture decane-
61 heptane-pentane and the quaternary mixture decane-heptane-pentane-methane, at two
62 pressures and at 50°C, will be studied on-board the Shijian-10 (SJ-10) Chinese satellite during
63 2016 (Galliero et al., 2015). To assure the success of this new mission, both validating ground
64 measurements and numerical simulations have been planned. In this paper we present results
65 on the iso-massic binary mixture decane-pentane based on the measurement of non-
66 equilibrium (NE) fluctuations.
67 In general, from the analysis of the dynamics of concentration NE fluctuations by light-
68 scattering it is possible to measure the fluid transport properties coefficients, including the
69 mass diffusion and Soret coefficients, as demonstrated for binary mixtures (Croccolo et al.,
70 2012, 2014). The technique has been adapted to high pressure (Giraudet et al., 2014). In this
71 work we extend the technique to the analysis of thermal fluctuations thus including the
72 possibility of measuring the thermal diffusivity coefficient of the mixture. Conversely, due to
73 the limited amplitude of the optical signal obtained for this system, we were not able here to
74 measure the Soret coefficient.
75 The remainder of the paper is organized as follows: Section 2 reports the methodology, in
76 Section 3 we provide results and discussion, and in Section 4 conclusions are drawn.
77

78 ## 2. Methodology

79

80 ***Theoretical background***

81 In a homogeneous multicomponent mixture a temperature gradient induces heat transfer as
82 well as segregation of the components along the temperature gradient by means of the Soret

effect (de Groot and Mazur, 1984). The segregation induces then Fickean diffusion and the combination of the two phenomena results in a steady concentration gradient which is convection-free only in microgravity conditions or in particular cases on ground. A thermodiffusion experiment on ground is typically performed by applying a stabilizing thermal gradient to a multicomponent fluid mixture, thus obtaining a superposition of the mentioned phenomena. Even if there is no total mass flux in the steady state, thermal and concentration NE fluctuations are always present. NE fluctuations are strictly related to the transport properties of the fluid. That is why from NE fluctuations analysis one can determine in principle all transport coefficients, like viscosity, thermal diffusivity and solutal diffusion and thermodiffusion coefficients. A detailed description of the theory of NE fluctuations can be found in the book by Ortiz de Zárate and Sengers (Ortiz de Zárate and Sengers, 2006). Here we briefly recall the essential equations that will be used in the following.

In a binary mixture, the temporal correlation function of NE concentration fluctuations induced by the Soret effect is expected to be a single exponential decay for all wave vectors, with time constants $\tau_S(q)$ varying as a function of the wave vector q. For wave vectors much larger than a characteristic value q_s^*, the decay time is the solutal diffusive one:

$$\tau_S(q) = 1/(Dq^2), \qquad \text{(Eq. 1)}$$

where D is the mass diffusion coefficient. NE thermal fluctuations are faster and overlap to the solutal ones. For wave vectors larger than a thermal characteristic wave vector q_T^*, the decay time is the thermal diffusive one:

$$\tau_T(q) = 1/(\kappa q^2), \qquad \text{(Eq. 2)}$$

where κ is the thermal diffusivity coefficient.

Experimental set-up

Our thermodiffusion cell (Fig.1 of Giraudet et al., 2014) is specifically designed for applying a vertical temperature gradient with excellent thermal homogeneity and stability to a horizontal slab of a multicomponent fluid under high pressure while providing vertical optical access to a central area of the cell. The cell core consists of a stainless steel annulus of internal/external diameter 30/75mm with high pressure inlet and outlet at its opposite sides. This part accommodates Teflon®-coated Viton® O-rings for sealing, and square sapphire plates kept at a distance L = 5mm by the annulus itself, thus defining the sample thickness. In order to minimize the contact between the liquid sample and the conductive metal a Teflon annulus (internal/external diameter 19.8/30mm) with two thin holes (diameter 1mm) for inlet/outlet of the fluid has been inserted in the inner part of the stainless annulus zone.

The external sides of the sapphire windows are in thermal contact with two aluminium plates with a central circular aperture (d=13mm), where two thermistors (Wavelenght Electronics, TCS651) are installed to monitor the sapphire temperatures. External to the aluminium plates, two Peltier elements (Kryotherm, TB-109-1.4-1.5 CH) with central circular aperture (d=13mm) provide/remove the heat necessary to maintain the set-point temperature as driven by two temperature controllers (Wavelenght Electronics, LFI-3751) maintaining the temperature of the internal side of each Peltier device with a stability better than 1mK RMS over 1 day. Finally, external to the Peltier elements, two aluminium plates are flushed with water coming from a thermostatic bath (Huber, ministat 125) to remove the excess heat of the Peltiers.

Experiments have been performed with the iso-massic binary mixture of decane (Sigma-Aldrich, ≥99%) and pentane (Sigma-Aldrich, ≥99%). Components were used without further

purification. The mixture is prepared in a bottle by weighting on a balance (Sartorius, TE313S, resolution 10^{-2}g/200g) first the decane and then the pentane. The bottle is carefully closed by cover with Teflon sealing. Error in mass fraction is estimated less than ±0.0001.

The filling system consists of: a rotary vacuum pump able to evacuate most of the air from the cell before filling operations down to a residual pressure of about 10Pa; a fluid vessel at atmospheric pressure; a manual volumetric pump and a number of valves to facilitate the procedure. Briefly, after a low vacuum is made inside the cell, the mixture to be studied is transferred to the cell by acting on the volumetric pump. Visual check allows avoiding bubbles during the injection procedure. After that, the cell is abundantly fluxed with the fluid mixture. At the end of the procedure a valve is closed and the volumetric pump is operated to modify the liquid pressure within the cell. A manometer (Keller, PAA-33X, pressure range: 0.1÷100MPa, precision ±0.04MPa) is connected between the volumetric pump and the cell to measure the pressure of the fluid mixture. A second identical manometer is connected to the outlet of the cell. The manometer signals are transferred using an acquisition card (National Instruments, NI 9215) interfaced to a computer.

We perform our experiments by imposing a difference of temperature ΔT on the horizontally positioned thin cell, previously filled with the homogenous fluid mixture.

In order to investigate NE fluctuations, it is common to use a scattering in the near field technique as the Shadowgraph (Wu et al. 1995), for which the physical optics treatment was given by Trainoff and Cannell (2002) and Croccolo and Brogioli (2011). The shadowgraph optical setup involves a low coherence light source (Super Lumen, SLD-MS-261-MP2-SM, λ = 675±13nm) that illuminates the bottom of the cell through a single-mode fiber. The diverging beam exiting from the fiber end is collimated by an achromatic doublet lens (f = 150mm, ϕ=50.8mm) and then passes through a linear film polarizer. In combination with a second linear polarizer after the cell the latter allows us to adapt the average light intensity.

The detection plane is located at about z = 95mm from the sample plane. As a sensor, we use a charge coupled device (AVT, PIKE-F421B) with 2048 ×2048 square pixels each of size 7.4 ×7.4μm^2 and a dynamic range of 14-bit. Images were cropped within a 768x768pix² in order to reach the maximum acquisition frame rate of the camera of about 30Hz.

Dynamic near-field imaging

Images acquired by means of a near-field scattering setup consist of an intensity map $I(\vec{x},t)$ generated by the interference on the CCD plane between the portion of the incident beam that has passed undisturbed through the sample and the beams scattered by refractive index fluctuations occurring within the sample (Trainoff and Cannell, 2002; Croccolo and Brogioli, 2011). Statistical analysis involving fast Fourier transforms provides accurate measurements of the intensity $I_s(\vec{q},t)$ of light scattered at each wave vector $\vec{q}$ grabbed by the optical setup and for all the times t of the acquisition sequence. Different setups show different responses to the acquired signal as a function of the wave number q, which is described by the so-called transfer function $T(q)$.

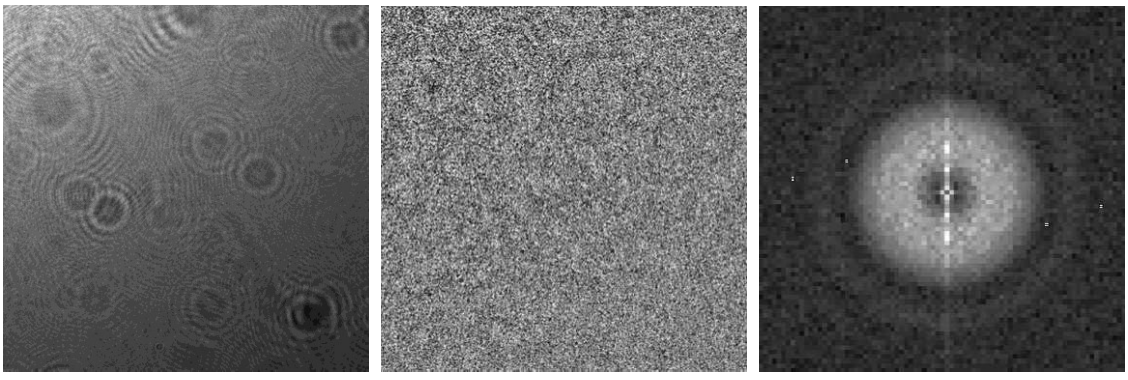

(a) ***(b)*** ***(c)***

Figure 1*: Results of a near field scattering experiment (shadowgraph layout) on the iso-massic binary of decane and pentane stressed by a thermal gradient (T_{mean} = 50°C, P = 20*

MPa, ΔT = 30°C).(a) 768×768 pix² near field image of the sample, $I(\vec{x},t)$ *(b) image difference,* $\Delta I(\vec{x},\Delta t) = I(\vec{x},t+\Delta t) - I(\vec{x},t)$*, having a correlation time of Δt =0.35 s and (c) 2D Fast Fourier Transform squared* $\left|I(\vec{q},t+\Delta t) - I(\vec{q},t)\right|^2$ *of (b).*

Details of the quantitative dynamic analysis can be found elsewhere (Croccolo et al., 2006a; Croccolo et al., 2006b; Croccolo et al., 2007; Cerchiari et al., 2012). Here we just recall that the quantity directly obtained from the experiments is the so-called structure function $C_m(q,\Delta t) = \left\langle \left|\Delta I_m(q,\Delta t)\right|^2 \right\rangle$, that is obtained by averaging (over all available times *t* in each image dataset and over the wave vector $\vec{q}$ azimuthal angle) the individual spatial Fourier transforms of the shadowgraph image differences, like the one shown in the example of Fig. 1. This experimental structure function is theoretically related to the temporal correlation function of NE composition fluctuations, also called intermediate scattering function (*ISF*), by:

$$C_m(q,\Delta t) = 2\{S(q)T(q)[1 - ISF(q,\Delta t)] + B(q)\}, \qquad \text{(Eq.3)}$$

with $ISF(q,0) = 1$. In Eq.3, $S(q)$ is the static power spectrum of the sample, $T(q)$ is the optical transfer function and $B(q)$ the background noise of the measurement. It is implicitly assumed in Eq.3 that the linear response of the CCD detector and any other electronic or electromagnetic proportionality parameters are aggregated inside $T(q)$ and/or $B(q)$.

3. Results and Discussion

Thermodynamic conditions

202 To determine the thermodynamic conditions of the study, we have calculated, with TOTAL
203 S.A. company BEST software, the biphasic envelop and critical coordinates of the iso-massic
204 binary mixture of decane and pentane. For a given pressure P and a given temperature T, the
205 software calculates the possible molar volumes v from the PPR78 equation of state (Peng and
206 Robinson, 1976). In Fig.2 we report the calculated biphasic envelop.
207

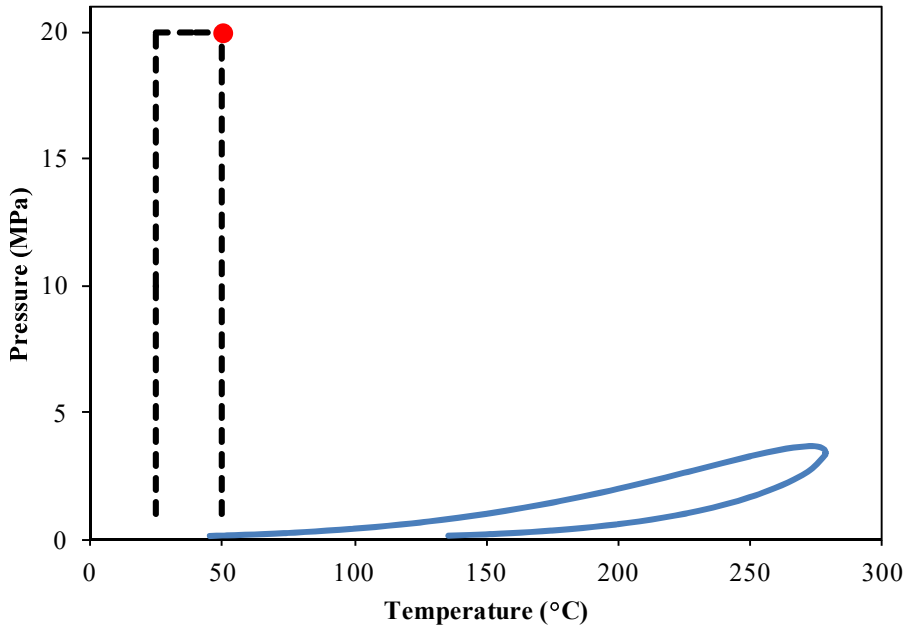

208
209 ***Figure 2****: Phase diagram of the isomassic binary mixture decane-pentane: the continuous*
210 *line represents the biphasic envelop. The dashed lines represent the values of pressure and*
211 *temperature investigated for the reported thermodiffusion experiments. The red point*
212 *indicates the thermodynamic conditions of the thermodiffusion experiment shown in Fig. 1, 3*
213 *and 4 (T_{mean} = 50°C, P = 20 MPa).*
214
215 In Fig.2 the dashed line represents the values of pressure and temperature investigated for
216 the present thermodiffusion experiments, the temperature of 50°C being imposed by the
217 microgravity experimental conditions of the SCCO project, and the temperature of 25°C
218 being selected as the experimental data references for mass diffusion coefficients only exist at

this temperature. Initially, a temperature difference of 20°C was applied to the system. To increase the optical signal, which remains low as revealed by Fig.1b-c, we applied a temperature difference of 30°C. In all the investigated conditions the mixture was in its liquid state, even at low pressure and for temperature differences of ΔT = 20 and 30°C. The red point in Fig.2 indicates the thermodynamic conditions of the thermodiffusion experiment shown in Fig.1, 3 and 4 (T_{mean} = 50°C, P = 20 MPa).

Structure function

At each investigated temperature T and pressure P, 10 different image acquisition runs have been performed with a delay time dt_{min} = 35ms between two consecutive images. Each set, containing 2000 images, has then been processed on a dedicated PC by means of a custom-made CUDA/C++ software (Cerchiari et al., 2012), in order to perform a fast parallel processing of the images to obtain the structure functions $C_m(q,\Delta t)$, for all the wave numbers and for all the correlation times accessible within the image datasets. In each experiment the temperature gradient is applied via two distinct temperature controllers, so that a linear temperature gradient sets up in some tens of seconds. The image acquisition is started about five hours later, to be sure that the concentration gradient due to the Soret effect is fully developed within the cell.

In Fig.3 we present the mean structure function $C_m(q,\Delta t)$ of the 10 runs a) as a function of the wave number for different correlation times and b) as a function of the correlation time for different wave numbers, for mean temperature T_{mean} = 50°C, pressure P = 20MPa and a difference of temperature ΔT = 30°C. The oscillatory behavior shown in Fig.3a is due to the optical transfer function $T(q)$ (see Eq.3). It is typical of shadowgraph experiments and it corresponds to the ring pattern shown in Fig. 1c.

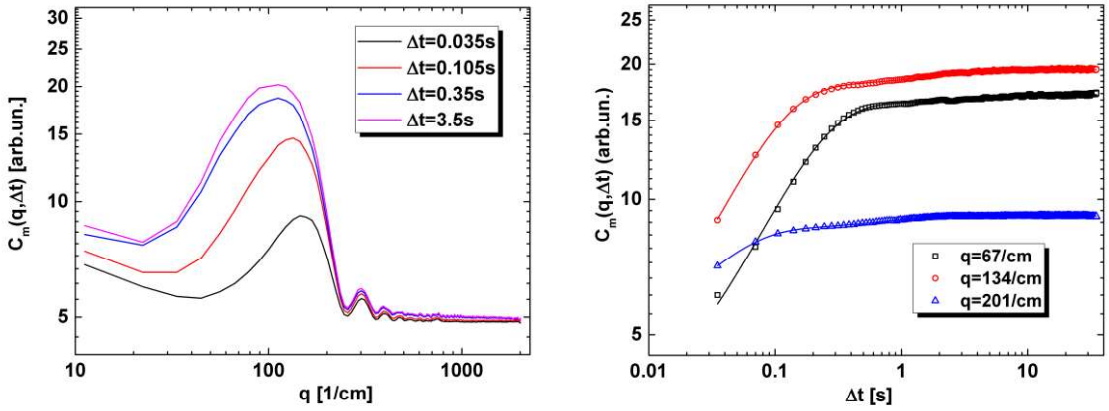

(a) (b)

***Figure 3**: Experimental structure function $C_m(q,\Delta t)$ (a) as a function of the wave vector q for different correlation times Δt and (b) as a function of the correlation time Δt for different wave vectors q (T_{mean} = 50°C, P = 20MPa, ΔT = 30°C).*

Fig.3a shows that for wave numbers q > 400cm^{-1}, the signal is completely lost in the background noise. For intermediate wave numbers, Fig.3b shows that the time dependence of the structure function cannot be totally assumed mono-exponential, as it is visible for wave numbers q = 134cm^{-1} and 201cm^{-1}. To account for the solutal relaxation mode plus the thermal relaxation mode, we therefore decided to perform a quantitative analysis of the experimental structure functions by modeling the *ISF* as a double exponential decay, namely:

$$ISF(q,\Delta t) = a\exp\left(-\frac{\Delta t}{\tau_1(q)}\right)+(1-a)\exp\left(-\frac{\Delta t}{\tau_2(q)}\right), \qquad \text{(Eq. 4)}$$

where τ_1 and τ_2 are two relaxation times. Hence, we performed fittings of the experimental $C_m(q,\Delta t)$ as a function of Δt (see Fig.3b) by substituting Eq.4 into Eq.3 and adopting as fitting

parameters: the product $S(q)T(q)$, the background $B(q)$, the relative amplitude *a*, and the two decay times, τ_1 and τ_2. For the fitting procedure we used a Levenberg-Marquardt Non-Linear Least Square fitting algorithm.

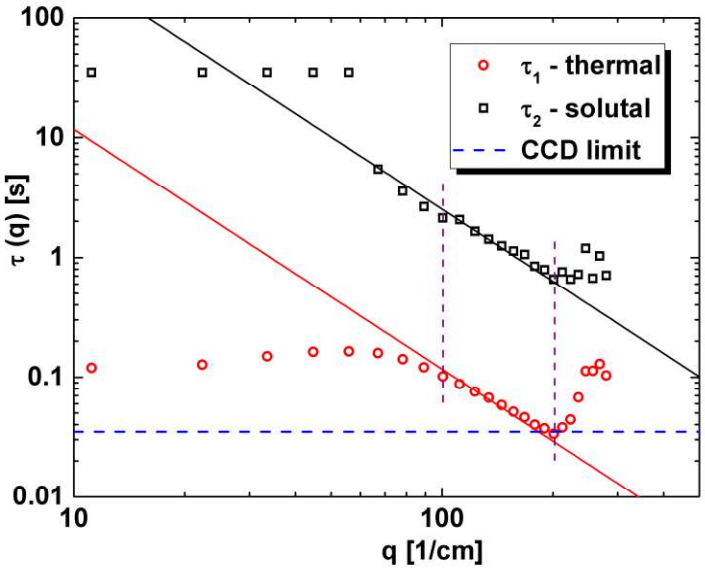

Figure 4*: Experimental decay times of NE fluctuations as obtained by fitting through Eqs.3 and 4, as a function of the wave number q. ○: fast mode, □: slow mode (T_{mean} = 50°C, P = 20MPa, ΔT = 30°C). The black solid line represents the theoretical relaxation times $1/Dq^2$ of Eq.1 and the red solid line represents the theoretical relaxation times $1/\kappa q^2$ of Eq.2.*

In Fig.4 we show the two decay times obtained from modeling the *ISF* by Eq.4, as a function of the wave number. The horizontal dashed blue line corresponds to $dt_{\min}$ = 35ms, which is the physical limit of our experimental recording equipment.

Intuitively, we assumed that the fastest mode was associated with a thermal mode and the slowest to a solutal mode.

In the range of wave numbers $100\,cm^{-1} \le q \le 200\,cm^{-1}$ (vertical dotted lines are plotted in Fig.4 to guide the reader) the slowest mode was fitted with Eq.1 using *D* as free parameter and the

fastest was fitted with Eq.2 using κ as free parameter. The results of the adjustments are reported by continuous lines in Fig.4. For example, referring to the conditions of Fig.4 (P = 20MPa, T_{mean} = 50°C) the two values obtained by fitting are D = (38±4)x10^{-6}cm^2/s and κ = (870±40)x10^{-6}cm^2/s. Uncertainties are the average of the deviations respect to the mean value of the 10 measurements.

Mass diffusion and thermal diffusivity coefficients

In Fig.5 we report the values of mass diffusion and thermal diffusivity coefficients as a function of the pressure obtained for the iso-massic binary mixture of decane and pentane, at T_{mean} = 25°C and for a temperature difference ΔT = 20°C.

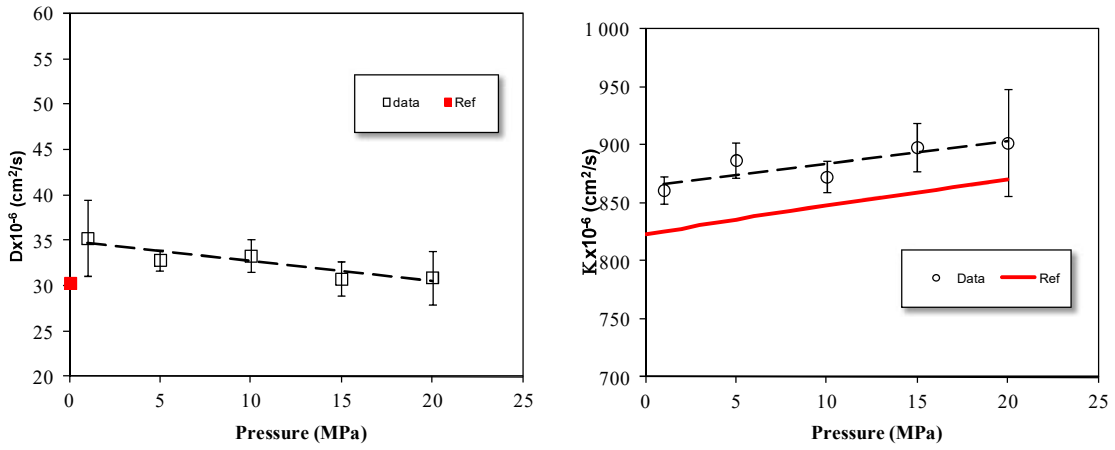

(a) (b)

Figure 5: *Mass diffusion D and thermal diffusivity κ coefficients as a function of the pressure at T_{mean}= 25°C and for a temperature difference of ΔT = 20°C.*

We found only one reference value of the mass diffusion coefficients at atmospheric pressure (Alonso De Mezquia et al., 2012) that we reported in Fig.5a as a red point. The thermal

297 diffusivity coefficients were compared with values found in NIST data base (NIST website)
298 and reported by a red continuous line in Fig.5b. Our values slightly overestimate reference
299 values. However, over the entire pressure range studied, the relative deviation of the thermal
300 diffusivity coefficients values does not exceed 5%. These results validate our hypothesis for
301 the interpretation of the modes of the measured intermediate scattering function, namely that
302 the fastest mode is the thermal relaxation mode of NE fluctuations and the slowest a mass
303 relaxation mode.
304 In Fig.5a we can notice a slight linear decrease in the mass diffusion coefficient with pressure
305 that is consistent with an increase of the viscosity with pressure (mass diffusion coefficient
306 being proportional to the inverse of the viscosity), as it has been shown in Alonso De Mezquia
307 et al., 2012. Also in Fig.5b we can see a linear increase in the thermal diffusivity coefficients
308 with pressure that is consistent with an increase of the density with pressure.
309 In Figure 6 we report the values of mass diffusion and thermal diffusivity coefficients as a
310 function of the mean temperature obtained for the iso-massic binary mixture of decane and
311 pentane, at P = 20MPa and for a temperature difference ΔT = 30°C.
312

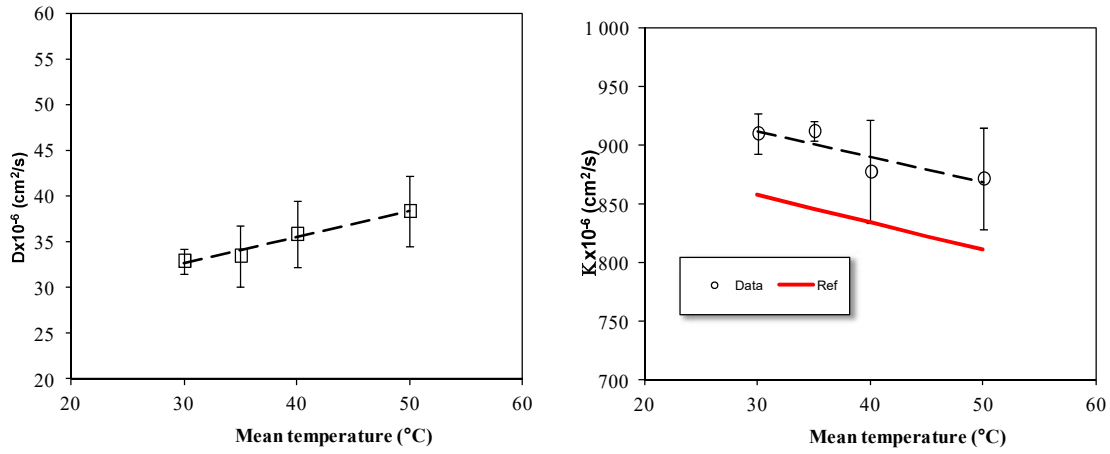

313
314 (a) (b)

Figure 6: *Mass diffusion D and thermal diffusivity κ coefficients as a function of the mean temperature at P= 20MPa and for a temperature difference of ΔT = 30°C.*

In Fig.6a we can see that the mass diffusion coefficient increases with the mean temperature, which is consistent with a decrease of the viscosity of the system with the mean temperature. In Fig.6b we can see that the thermal diffusivity coefficient decreases with the mean temperature. Again an overestimate of the reference values is detected.

In Fig.7 we report the values of mass diffusion and thermal diffusivity coefficients as a function of the pressure obtained for the iso-massic binary mixture of decane and pentane, at T_{mean} = 50°C and for a temperature difference ΔT = 30°C. The same trends as for Fig.5 are observed.

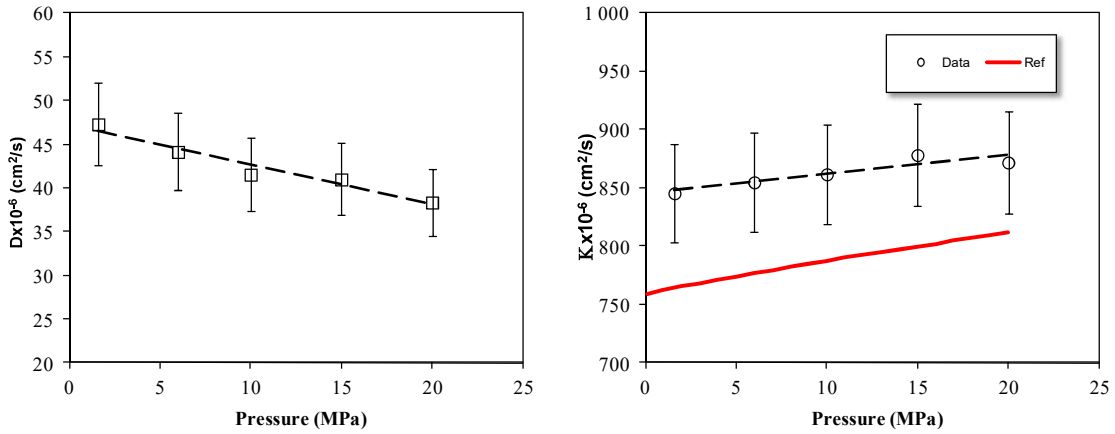

Figure 7: *Mass diffusion D and thermal diffusivity κ coefficients as a function of the pressure at T_{mean}= 50°C and for a temperature difference of ΔT = 30°C.*

4. Conclusions

Thermodiffusion experiments on iso-massic binary mixture of decane and pentane, in the liquid phase, have been performed between 25°C and 50°C and for pressures from 1MPa until 20MPa. By means of dynamic analysis of the light scattered by concentration NE fluctuations of the binary mixture we obtained the values of the mass diffusion coefficient D at each temperature and pressure. The shadowgraph set-up and its acquisition chain enabled us to achieve a minimum delay time between two successive images of 35ms. We were thus able to investigate for the first time temperature NE fluctuations, which let us model the ISF as the sum of two decreasing exponentials. This procedure allowed obtaining simultaneously the values of the thermal diffusivity coefficient κ. Mass diffusion coefficients D decrease with the pressure while thermal diffusivity coefficients κ increase with the pressure. For the investigated mixture, due to a limited intensity of the optical signal, it was not possible to obtain a reliable measurement of the Soret coefficients S_T. Therefore the obtained values of the mass diffusion coefficients D must be combined with thermodiffusion coefficients D_T measurements obtained by an independent experiment, such as thermogravitational column. The resulting values at 50°C can be directly compared to measurements made in microgravity in the frame of the SCCO-SJ10 project**.**

Acknowledgements

This work has been supported by the European Space Agency through the SCCO project. Support from the French space agency CNES is also acknowledged. We thank TOTAL S.A. for allowing the use of the BEST software and Research Groups (No. IT1009-16) and TERDISOMEZ (No. FIS2014-58950-C2-1-P) of MINECO.

References

- Alonso de Mesquia, D., Bou-Ali, M.M., Larrañage, M., Madariaga, J.A., Santamaria, C.: Determination of molecular diffusion coefficient in n-alkane binary mixtures: Empirical correlations. J. Phys. Chem. B 116, 2814-2819 (2012).
- Assael, M.J., Goodwin, A.R.H., Vesovic, V., Wakeham, W.A.: Experimental Thermodynamics Volume IX: Advances in Transport Properties of Fluids, Royal Society of Chemistry, London, (2014).
- Bou-Ali, M.M., Ahadi, A., Alonso de Mezquia, D., Galand, Q., Gebhardt, M., Khlybov, O., Köhler, W., Larrañaga, M., Legros, J.C., Lyubimova, T., Mialdun, A., Ryzhkov, I., Saghir, M.Z., Shevtsova, V., Van Vaerenbergh, S.: Benchmark values for the Soret, thermodiffusion and molecular diffusion coefficients of the ternary mixture tetralin+isobutylbenzene+n-dodecane with 0.8-0.1-0.1 mass fraction. Eur. Phys. J. E 38, 30 (2015).
- Cerchiari, G., Croccolo, F., Cardinaux, F., Scheffold, F.: Quasi-real-time analysis of dynamic near field scattering data using a graphics processing unit. Rev. Sci. Instrum. 83, 106101 (2012).
- Croccolo, F., Brogioli, D., Vailati, A., Giglio, M., Cannell, D.S.: Use of the dynamic Schlieren to study fluctuations during free diffusion. App. Opt. 45, 2166-2173 (2006a).
- Croccolo, F., Brogioli, D., Vailati, A., Giglio, M., Cannell, D.S.: Effect of gravity on the dynamics of non equilibrium fluctuations in a free diffusion experiment. Ann. N. Y. Acad. Sci. 1077, 365 (2006b).
- Croccolo, F., Brogioli, D., Vailati, A., Giglio, M., Cannell, D.S.: Non-diffusive decay of gradient driven fluctuations in a free-diffusion process. Phys. Rev. E. 76, 41112 (2007).

- Croccolo, F., Brogioli, D.: Quantitative Fourier analysis of schlieren masks: the transition from shadowgraph to schlieren. App. Opt. 50, 3419-3427 (2011).
- Croccolo, F., Bataller, H., Scheffold, F.: A light scattering study of non equilibrium fluctuations in liquid mixtures to measure the Soret and mass diffusion coefficient. J. Chem. Phys. 137, 234202 (2012).
- Croccolo, F., Bataller, H., Scheffold, F.: Static versus dynamic analysis of the influence of gravity on concentration non equilibrium fluctuations. Eur. Phys. J. E 37, 105 (2014).
- de Groot, S.R., Mazur, P: *Nonequilibrium Thermodynamics*. Dover, New York (1984).
- Firoozabadi, A., Ghorayeb, K., Shukla, K.: Theoretical model of thermal diffusion factors in multicomponent mixtures, AIChE Journal 46, 892-900, 2000.
- Galliero, G., Duguay, B., Caltagirone, J.P., Montel, F.: On thermal diffusion in binary and ternary mixtures by non-equilibrium molecular dynamics, Phil. Mag. 83, 2097-2108 (2003).
- Galliero, G., Montel, F.: Understanding compositional grading in petroleum reservoirs thanks to molecular simulations. Society of Petroleum Engineers Paper. 121902, Amsterdam, 2009
- Galliero, G., Bataller, H., Croccolo, F., Vermorel, R., Artola, P.-A., Rousseau, B., Vesovic, V., Bou-Ali, M., Ortiz de Zárate, J.M., Xu, S., Zhang, K., Montel, F.: Impact of Thermodiffusion on the initial distribution of Species in hydrocarbon reservoirs. Microgravity Sci. Technol. DOI 10.1007/s12217-015-9465-6.
- Gebhardt M. and Köhler W.: Soret, thermodiffusion, and mean diffusion coefficients of the ternary mixture ndodecane+ isobutylbenzene+1,2,3,4 tetrahydronaphthalene. J. Chem. Phys. 143, 164511 (2015).

406 - Georis, P., Montel, F., Van Vaerenbergh, S., Decoly, Y., Legros, J.C.: Proceedings of
407 the European Petroleum Conference, 1, pp. 57-62 (1998).
408 - Ghorayeb, K., Firoozabadi, A., Anraku, T.: Interpretation on the unusual fluid
409 distribution in the Yufutsu gas-condensate field. SPE J. 8, 114-123 (2003).
410 - Giraudet, C., Bataller, H., Croccolo, F.: High-pressure mass transport properties
411 measured by dynamic near-field scattering of non-equilibrium fluctuations. Eur. Phys.
412 J. E 37, 107 (2014).
413 - Høier, L., Whitson, C.H.: Compositional grading-theory and Practice. SPE Reserv.
414 Evaluation Eng. 4, 525-532 (2001).
415 - Kempers L.J.T.M.: A comprehensive thermodynamic theory of the Soret effect in a
416 multicomponent gas, liquid, or solid, J. Chem. Phys. 115, 6330-6341 (2001).
417 - Larrañaga M., Bou-Ali M., Lizarraga I., Madariaga J.A., Santamaría S.: Soret
418 Coefficients of the Ternary Mixture 1,2,3,4-Tetrahydronaphthalene + Isobutylbenzene
419 + N-Dodecane, J. Chem. Phys. 143, 024202 (2015).
420 - Leahy-Dios, A., Bou-Ali, M.M., Platten, J.K., Firoozabadi, A.: Measurements of
421 molecular and thermal diffusion coefficients in ternary mixtures, J. Chem. Phys. 122,
422 234502 (2005).
423 - Lira-Galeana, C., Firoozabadi, A., Prausnitz, J.M.: Computation of compositional
424 grading in hydrocarbon reservoirs. Application of continuous thermodynamics. Fluid
425 Phase Equilib. 102, 143-158 (1994).
426 - Montel, F., Bickert, J., Lagisquet, A., Galliero, G.: Initial state of petroleum reservoirs:
427 A comprehensive approach. J. Pet. Sci. Eng. 58, 391-402 (2007).
428 - NIST website: http://webbook.nist.gov/chemistry/
429 - Ortiz de Zárate J.M., Sengers, J.V.: Hydrodynamic Fluctuations in Fluids and Fluid
430 Mixtures, Elsevier, Amsterdam, (2006).

- Peng, D.Y., Robinson, D.B.: A new two-constant equation of state. Ind. Eng. Chem. Fundam. 15, 59-64 (1976).
- Srinivasan, S., Saghir, M.Z.: Measurements on thermodiffusion in ternary hydrocarbon mixtures at high pressure. J. Chem. Phys. 131, 124508 (2009).
- Trainoff, S.P., Cannell, D.S.: Physical optics treatment of the shadowgraph. Phys. of Fluids 14, 1340-1363 (2002).
- Touzet, M., Galliero, G., Lazzeri, V., Saghir, M.Z., Montel, F., Legros, J.C.: Thermodiffusion: from microgravity experiments to the initial state of petroleum reservoirs, Comptes Rendus - Mécanique 339, 318-323 (2011).
- VanVaerenbergh, S., Srinivasan S., Saghir, M.Z.: Thermodiffusion in multicomponent hydrocarbon mixtures: Experimental investigations and computational analysis. J. Chem. Phys. 131, 114505 (2009).
- Wu, M., Ahlers, G., Cannell, D.S.: Thermally induced fluctuations below the onset of the Rayleigh-Bénard convection. Phys. Rev. Lett. 75, 17432-1746 (1995).